

Synthesis, Characterization, and Electrochemical Behavior of Mono- and Bimetallic Ruthenium and Rhenium Allenylidenes Bearing Multiconjugated Organic Spacers

Nicoletta Mantovani,[†] Michele Brugnati,[†] Luca Gonsalvi,[‡] Emanuela Grigiotti,[§] Franco Laschi,[§] Lorenza Marvelli,^{*,†} Maurizio Peruzzini,^{*,‡} Gianna Reginato,^{*,§} Roberto Rossi,[†] and Piero Zanello^{*,§}

Laboratorio di Chimica Nucleare ed Inorganica, Dipartimento di Chimica, Università di Ferrara, Via L. Borsari 46, 44100 Ferrara, Italy, Consiglio Nazionale delle Ricerche, Istituto di Chimica dei Composti Organometallici (ICCOM-CNR), Via Madonna del Piano, 50019 Sesto Fiorentino (Firenze), Italy, and Dipartimento di Chimica, Università di Siena, Via Aldo Moro, 53100 Siena, Italy

Received October 8, 2004

Novel monoallenylidenes of Ru and Re and homobimetallic Ru/Ru and heterobimetallic Ru/Re complexes bridged by multiconjugated aromatic organic spacers such as bianthracenylidene and biphenylene were obtained and characterized by conventional spectroscopic techniques and elemental analysis. Electrochemical measurements coupled to spectroelectrochemistry and EPR spectroscopy proved that in the bis(allenylidene) complexes an electronic communication is present between either the two allenylidene bridges or the two metal centers, entailing extended intramolecular electronic mobility.

Introduction

The chemistry and reactivity of transition metal allenylidenes^{1,2} and higher cumulenes³ is well documented and has received renewed interest due to the many different applications, ranging from homogeneous catalysis⁴ to molecular materials, such as sensors and wires⁵ and liquid crystals.^{6–8}

A major step forward in the synthesis of transition metal allenylidenes was achieved by Selegue, who showed that Ru(II) complexes readily react with propargylic alcohols to yield, via a metal-mediated π -alkyne to vinylidene tautomerization, a generally transient hydroxyvinylidene. Intramolecular elimination of water from the latter leaves the $M=C(\alpha)=C(\beta)=C(\gamma)$ allenylidene moiety.⁹ Many contributions to the chemistry and reactivity of this class of organometallic compounds, particularly of ruthenium, are reported in the literature, for example through further functionalization of the unsaturated chain which can undergo attack by both nucleophiles on C(α) and C(γ) and electrophiles on C(β).^{2,10} Protection of C(α) is normally achieved by the use of bulky monodentate ligands or diphosphines, which shield this carbon atom against nucleophilic attack and therefore increase the selectivity of the organometallic reaction. Kinetic rather than thermo-

dynamic preference for the attack at C(γ) by nucleophiles, such as amines and phosphines, has been documented, and a few examples of C(γ) to C(α) rear-

(4) (a) Nishibayashi, Y.; Yoshikawa, M.; Inada, Y.; Hidai, M.; Uemura, S. *J. Am. Chem. Soc.* **2002**, *124*, 11846. (b) Saoud, M.; Mañas Carpio, S.; Romerosa, A.; Gonsalvi, L.; Peruzzini, M. *Eur. J. Inorg. Chem.* **2003**, 1614. (c) Fürstner, A.; Picquet, M.; Bruneau, C.; Dixneuf, P. H. *Chem. Commun.* **1998**, 1315. (d) Schanz, H. J.; Jafarpour, L.; Stevens, E. D.; Nolan, S. P. *Organometallics* **1999**, *18*, 5187. (e) Picquet, M.; Touchard, D.; Bruneau, C.; Dixneuf, P. H. *New J. Chem.* **1999**, *23*, 141. (f) Saoud, M.; Romerosa, A.; Peruzzini, M. *Organometallics* **2000**, *19*, 4005. (g) Fürstner, A.; Liebl, M.; Lehmann, C. W.; Picquet, M.; Kunz, R.; Bruneau, C.; Touchard, D.; Dixneuf, P. H. *Chem. Eur. J.* **2000**, *6*, 1847. (h) Osipov, S. N.; Artyushin, O. I.; Kolomiets, A. F.; Bruneau, C.; Dixneuf, P. H. *Synlett* **2000**, *7*, 1031. (i) Osipov, S. N.; Artyushin, O. I.; Kolomiets, A. F.; Bruneau, C.; Picquet, M.; Dixneuf, P. H. *Eur. J. Org. Chem.* **2001**, 3891. (j) Jung, S.; Brandt, C. D.; Werner, H. *New J. Chem.* **2001**, *25*, 1101. (k) Çetinkaya, B.; Demir, S.; Özdemir, I.; Toupet, L.; Bruneau, C.; Dixneuf, P. H. *New J. Chem.* **2001**, *25*, 519. (l) Sémeril, D.; Oliver-Borbignon, H.; Bruneau, C.; Dixneuf, P. H. *Chem. Commun.* **2002**, 146. (m) Sémeril, D.; Bruneau, C.; Dixneuf, P. H. *Adv. Synth. Catal.* **2002**, *344*, 585. (n) Castarlenas, R.; Sémeril, D.; Noels, A. F.; Demonceau, A.; Dixneuf, P. H. *J. Organomet. Chem.* **2002**, *663*, 235. (o) Abdallaoui, I. A.; Sémeril, D.; Dixneuf, P. H. *J. Mol. Catal. A: Chem.* **2002**, *182–183*, 577. (p) Csihony, S.; Fischmeister, C.; Bruneau, C.; Horváth, I. T.; Dixneuf, P. H. *New J. Chem.* **2002**, *25*, 1667. (q) le Gendre, P.; Picquet, M.; Richard, P.; Moïse, C. *J. Organomet. Chem.* **2002**, *643–644*, 231. (r) Akiyama, R.; Kobayashi, S. *Angew. Chem., Int. Ed.* **2002**, *41*, 2602. (s) Nishibayashi, Y.; Inada, Y.; Hidai, M.; Uemura, S. *J. Am. Chem. Soc.* **2003**, *125*, 6060. (t) Castarlenas, R.; Dixneuf, P. H. *Angew. Chem., Int. Ed.* **2003**, *42*, 4524.

(5) (a) Constable, E. C. *Angew. Chem., Int. Ed. Engl.* **1995**, *30*, 21. (b) Bunz, U. H. F. *Angew. Chem., Int. Ed. Engl.* **1996**, *35*, 969. (c) Paul, F.; Lapinte, C. *Coord. Chem. Rev.* **1998**, *178*. (d) Dembinski, R.; Bartik, T.; Bartik, B.; Jaeger, M.; Gladysz, J. A. *J. Am. Chem. Soc.* **2000**, *122*, 810.

(6) Altmann, M.; Enkelmann, V.; Lieser, G.; Bunz, U. H. F. *Adv. Mater.* **1995**, *7*, 726.

(7) Takahashi, S.; Takai, Y.; Morimoto, H.; Sonogashira, K. *J. Chem. Soc., Chem. Commun.* **1984**, 3.

(8) Dembek, A. A.; Burch, R. R.; Feiring, A. E. *J. Am. Chem. Soc.* **1993**, *115*, 2087.

(9) Selegue, J. P. *Organometallics* **1982**, *1*, 217.

* Corresponding author. E-mail: mg1@unife.it, gianna.reginato@iccom.cnr.it; mperuzzini@iccom.cnr.it; zanello@unisi.it.

[†] Università di Ferrara.

[‡] Istituto di Chimica dei Composti Organometallici.

[§] Università di Siena.

(1) (a) Bruce, M. I. *Chem. Rev.* **1998**, *98*, 2797. (b) Winter, R. F.; Zális, S. *Coord. Chem. Rev.* **2004**, *248*, 1565.

(2) Cadierno, V.; Gamasa, M. P.; Gimeno, J. *Eur. J. Inorg. Chem.* **2001**, 571.

(3) Bruce, M. I. *Coord. Chem. Rev.* **2004**, *248*, 1603.

rangement have been reported for some rhenium(I) allenylidene adducts of nucleophiles.¹¹

Organoruthenium complexes with π -conjugated bridges have great importance for building molecular scale electronic devices that allow exchange of electrons through bridges between remote terminal groups. The redox aptitude of metallacumulenes,^{12–17} particularly of ruthenium(II) allenylidenes, is well documented. Both mononuclear^{14–17} and dinuclear¹² Ru=C=C=CR¹R² assemblies have been investigated probably because, contrary to most metal ions, the Ru(II) center seems to favor intramolecular electronic mobility when interposed between unsaturated carbon chains.¹⁷ In contrast, rhenium complexes linked to sp-carbon chains are less well studied.¹³ The extent of electron exchange between metal centers is usually assessed by cyclic voltammetry (CV)¹⁸ or, in case of complexes undergoing one-electron oxidation, by electron spin resonance (ESR) experiments.^{19a}

A variety of conjugated bridges and different synthetic methodologies have been used to connect two or more Ru units. Chart 1 shows examples of coupling of allenylidene and diynylmetal complexes to form a bimetallic Ru system with a C₇ conjugated bridge (**I**),¹⁸ the use of bifunctionalized propargylic alcohols to prepare bimetallic bis(allenylidene) derivatives (**II**),^{19b} their reversible deprotonation/protonation at the C(δ) atom to yield at first mixed allenylidene-alkenyl carbyne complexes (**III**) and then bis(alkenylcarbyne) ruthenium species (**IV**),^{19b,20} and the insertion of 3-ene-1,5-diynes into a Ru–H bond to give polyunsaturated (CH)₆-bimetallic complexes (**V**).²³ Polymetallic vinylidene and

allenylidene ruthenium complexes were also obtained by Dixneuf and co-workers via the Selegue protocol using dendrimers bearing either conjugated or nonconjugated terminal polyalkynes, yielding trimetallic complexes in the form of an organometallic “triskelion” (**VI**).^{24,25}

Worth noting is also the recent result by Rigaut et al., who were able to synthesize *trans*-[(dppe)₂Ru{C=C=CPh₂}][B(C₆F₅)₄]₂ (**I**) by an oxidative pathway encompassing the reaction of Ce(IV) ammonium nitrate with *trans*-[(dppe)₂Ru{C=C=CPh₂}]{C≡CCHPh₂}[B(C₆F₅)₄]₂ (**VII**).¹⁷ Complex **1** represents the first documented example of a metal-centered bis(allenylidene) species and is characterized by two one-electron reversible reduction waves.

Recently, we have shown that rhenium(I) forms stable vinylidenes and allenylidenes,²⁶ which in part parallel the chemistry and reactivity of the isoelectronic d⁶ ruthenium(II) carbenes but also exhibit unusual reactivity patterns unknown for the related Ru(II) derivatives.¹¹ Dirhenium and mixed heterodimetallic bis(allenylidene) derivatives containing bridging unsaturated carbenes are virtually unknown.²⁷ Intrigued by the possibility of using the highly versatile and stable [(triphos)Re(CO)₂]⁺ synthon to generate homo- and heteroconjugated bimetallic complexes with bridging unsaturated carbenes, we decided to examine whether bifunctional propargylic alcohols may be used to enter this class of compounds by expanding the original approach of Dixneuf and co-workers.^{19b}

Hereby we report our first results in this area describing the synthesis of monoallenylidenes of Ru and Re and of the corresponding novel homobimetallic Ru/Ru and heterobimetallic Ru/Re bis(allenylidenes) bridged by multiconjugated aromatic organic spacers, which were obtained by conversion of diketones such as [9,9′]-bianthracenylidene-10,10′-dione and (4-benzoylphenyl)phenyl methanone into their bis(propargylic) derivatives **L**₁ and **L**₂, respectively. Electrochemical and spectroelectrochemical measurements were carried out on selected bis(allenylidene) derivatives in order to highlight the presence of electronic communication

(10) Recent important references addressing the stoichiometric reactivity of metal allenylidenes include: (a) Mantovani, N.; Marvelli, L.; Rossi, R.; Bianchini, C.; de los Ríos, I.; Romerosa, A.; Peruzzini, M. *J. Chem. Soc., Dalton Trans.* **2001**, 2353. (b) Bustelo, E.; Jiménez-Tenorio, M.; Mereiter, K.; Puerta, M. C.; Valerga, P. *Organometallics* **2002**, *21*, 1903. (c) Cadierno, V.; Conejero, S.; Gamasa, M. P.; Gimeno, J.; Favello, L. R.; Llusar, R. M. *Organometallics* **2002**, *21*, 3716. (d) Cadierno, V.; Conejero, S.; Gamasa, M. P.; Gimeno, J. *Organometallics* **2002**, *21*, 3837. (e) Conejero, S.; Diez, J.; Gamasa, M. P.; Gimeno, J.; García-Granda, S. *Angew. Chem., Int. Ed.* **2002**, *41*, 3439. (f) Esteruelas, M. A.; López, A. M. In *Recent Advances in Hydride Chemistry*; Peruzzini, M.; Poli, R., Eds.; Elsevier SA: Amsterdam, 2001; p 189, and references therein. (g) Bernard, D. J.; Esteruelas, M. A.; López, A. M.; Oliván, M.; Oñate, E.; Puerta, M. C.; Valerga, P. *Organometallics* **2000**, *19*, 4327. (h) Baya, M.; Buil, M. L.; Esteruelas, M. A.; López, A. M.; Oñate, E.; Rodríguez, J. R. *Organometallics* **2002**, *21*, 1841. (i) Buil, M. I.; Esteruelas, M. A.; López, A. M.; Oñate, E. *Organometallics* **2003**, *22*, 162, and references therein. (j) Bertolasi, V.; Mantovani, N.; Marvelli, L.; Rossi, R.; Akbayeva, D. N.; Bianchini, C.; de los Ríos, I.; Peruzzini, M. *Inorg. Chim. Acta* **2003**, *344*, 207.

(11) (a) Mantovani, N.; Marvelli, L.; Rossi, R.; Bertolasi, V.; Bianchini, C.; de los Ríos, I.; Peruzzini, M. *Organometallics* **2002**, *21*, 2382. (b) Peruzzini, M.; Barbaro, P.; Bertolasi, V.; Bianchini, C.; de los Ríos, I.; Mantovani, N.; Marvelli, L.; Rossi, R. *J. Chem. Soc., Dalton Trans.* **2003**, 4121.

(12) Guesmi, S.; Touchard, D.; Dixneuf, P. H. *Chem. Commun.* **1996**, 2773.

(13) Brady, M.; Weng, W.; Zhou, Y.; Seiler, J. W.; Amoroso, A. J.; Arif, A. M.; Böhme, M.; Frenking, G.; Gladysz, J. A. *J. Am. Chem. Soc.* **1997**, *119*, 775.

(14) Rigaut, S.; Maury, O.; Touchard, D.; Dixneuf, P. H. *Chem. Commun.* **2001**, 373.

(15) Winter, R. F.; Klinkhammer, K.-W.; Zališ, S. *Organometallics* **2001**, *20*, 1317.

(16) Winter, R. F.; Hartmann, S.; Zališ, S.; Klinkhammer, K.-W. *Dalton Trans.* **2003**, 2342.

(17) Rigaut, S.; Costuas, K.; Touchard, D.; Saillard, J.-Y.; Golhen, S.; Dixneuf, P. H. *J. Am. Chem. Soc.* **2004**, *126*, 4072.

(18) Rigaut, S.; Massue, J.; Touchard, D.; Fillaut, J.-L.; Golhen, S.; Dixneuf, P. H. *Angew. Chem., Int. Ed.* **2002**, *41*, 4513.

(19) (a) Rigaut, S.; Monnier, F.; Mousset, F.; Touchard, D.; Dixneuf, P. H. *Organometallics* **2002**, *21*, 2654. (b) Rigaut, S.; Touchard, D.; Dixneuf, P. H. *Organometallics* **2003**, *22*, 3980.

(20) This transformation, reflecting the well-known reactivity of allenylidenes toward bases and acids, has been demonstrated by the sequential protonation of the bridged ruthenium complex *trans*-[Cl(dppe)₂Ru=C=C=C(CH₃){ μ -(*p*-C₆H₄)}(CH₃)C=C=C=Ru(dppe)₂Cl](BF₄)₂, which first results in *trans*-[Cl(dppe)₂Ru=C=C=C(CH₃){ μ -(*p*-C₆H₄)}(CH₃)C=C=C=Ru(dppe)₂Cl](BF₄)₂ and then in *trans*-[Cl(dppe)₂Ru=C=C=C(CH₃){ μ -(*p*-C₆H₄)}(CH₃)C=C=C=Ru(dppe)₂Cl](BF₄)₂.^{19b,21,22}

(21) Touchard, D.; Haquette, P.; Guesmi, S.; Le Pichon, L.; Daridor, A.; Toupet, L.; Dixneuf, P. H. *Organometallics* **1997**, *16*, 3640.

(22) Touchard, D.; Haquette, P.; Daridor, A.; Romero, A.; Dixneuf, P. H. *Organometallics* **1998**, *17*, 3844.

(23) Liu, S. H.; Xia, H.; Wen, T. B.; Zhou, Z.; Jia, G. *Organometallics* **2003**, *22*, 737.

(24) Uno, M.; Dixneuf, P. H. *Angew. Chem., Int. Ed.* **1998**, *37*, 1714.

(25) Weiss, D.; Dixneuf, P. H. *Organometallics* **2003**, *22*, 2209.

(26) (a) Bianchini, C.; Marchi, A.; Marvelli, L.; Peruzzini, M.; Romerosa, A.; Rossi, R. *Organometallics* **1996**, *15*, 3804. (b) Bianchini, C.; Marchi, A.; Mantovani, N.; Marvelli, L.; Masi, D.; Peruzzini, M.; Rossi, R. *Eur. J. Inorg. Chem.* **1998**, 211. (c) Bianchini, C.; Mantovani, N.; Marchi, A.; Marvelli, L.; Masi, D.; Peruzzini, M.; Rossi, R.; Romerosa, A. *Organometallics* **1999**, *18*, 4501. (d) Bianchini, C.; Mantovani, N.; Marvelli, L.; Peruzzini, M.; Rossi, R.; Romerosa, A. *J. Organomet. Chem.* **2001**, *617–618*, 233. (e) Peruzzini, M.; Barbaro, P.; Bertolasi, V.; Bianchini, C.; de los Ríos, I.; Mantovani, N.; Marvelli, L.; Rossi, R. *Dalton Trans.* **2003**, 4121.

(27) The dirhenium complex (*Re–Re*)-[Re(CO)₅Re(CO)₄]{C=C=C(Bu)₂} contains a terminal allenylidene ligand. See: Berke, H.; Härter, P.; Huttner, G.; Zsolnai, L. *Chem. Ber.* **1984**, *117*, 3423.

Chart 1

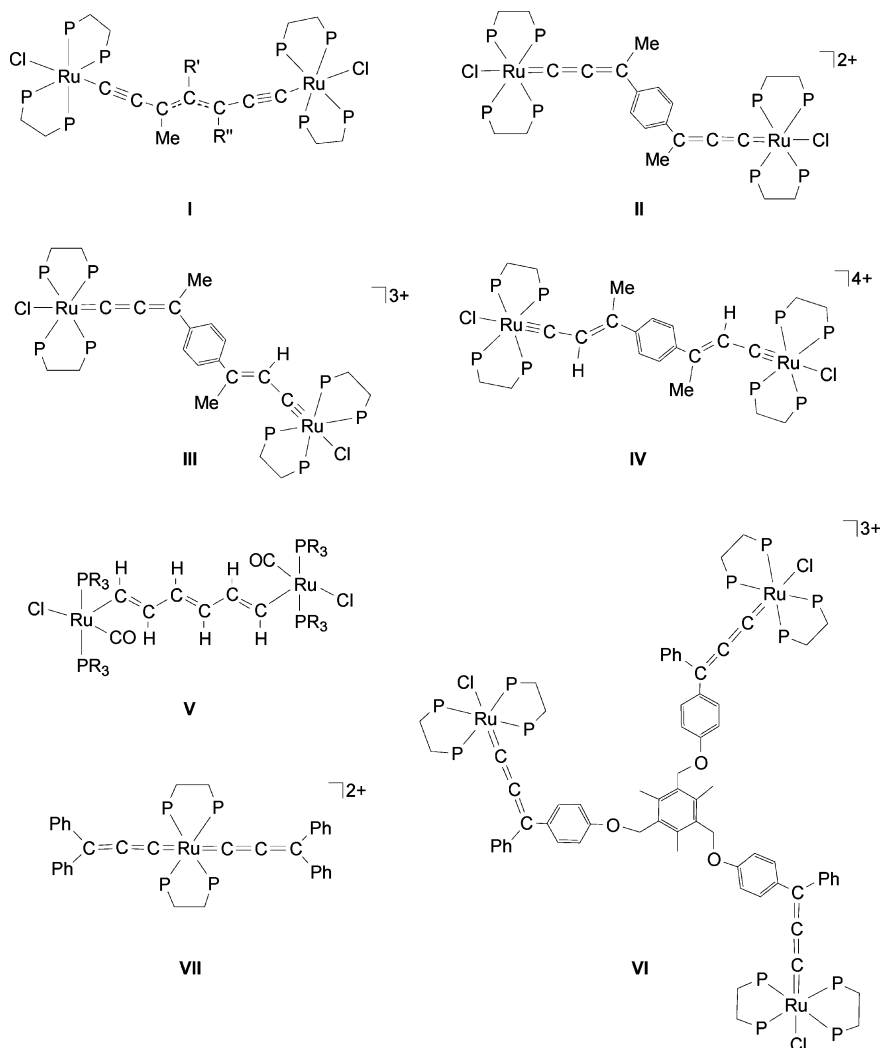
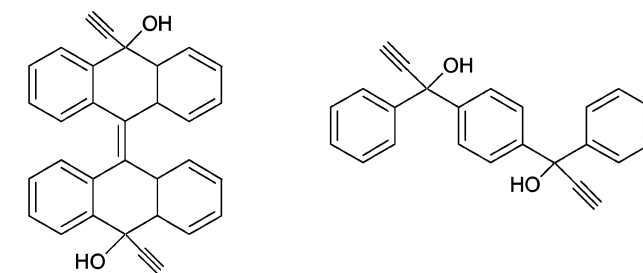
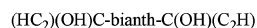


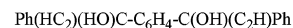
Chart 2



10,10'-Diethynyl-10H,10'H-[9,9']bianthracenylidene-10,10'-diol

L₁

1-[4-(1-Hydroxy-1-phenylprop-2-ynyl)-phenyl]-1-phenylprop-2-yn-1-ol

L₂

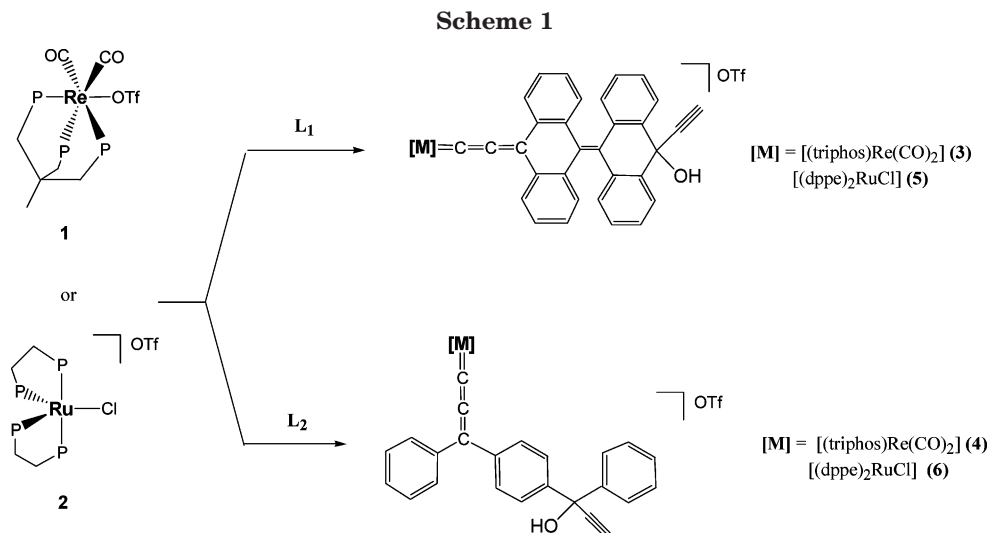
between the metal centers through the multiconjugated organic chains.

Results and Discussion

Synthesis and Characterization of Bis- α -alkynol Organic Spacers. The bis- α -alkynol ligands 10,10'-diethynyl-10H,10'H-[9,9']bianthracenylidene-10,10'-diol (**L₁**) and 1-[4-(1-hydroxy-1-phenylprop-2-ynyl)-phenyl]-1-phenylprop-2-yn-1-ol (**L₂**), shown in Chart 2, were prepared in excellent yields from the corresponding commercially available diketones via reaction with ethynylmagnesium chloride in THF at 60 °C. Addition of magnesium acetylides on carbonyl groups is a well-known procedure for obtaining propargylic alcohols, but was never described before on this kind of substrates. Early literature reports the synthesis of the related *trans*-9,10-diethynyl-9,10-dihydroanthracene-9,10-diol (**L₃**)²⁸ by addition of sodium acetylide although with incomplete characterization, whereas the two bispropargylic derivatives are unreported. Notably, compounds **L₁** and **L₂** were each obtained as a single diastereoisomer, likely bearing the alkynyl ends in *trans* configu-

ration in analogy with a *trans* addition as observed for **L₃**. The ¹H NMR spectra in CDCl₃ are indeed consistent with the proposed structures and show singlet resonances typical for the C≡CH proton at 2.86 and 2.85 ppm, respectively. In the same solvent the OH groups resonate at 2.92 and 3.04 ppm. The ¹³C{¹H} NMR spectra in the same solvent show singlets around 68 ppm (**L₁**) and 86 ppm (**L₂**) for C(OH)(C≡C), 74 ppm (**L₁**, **L₂**) for C≡CH, and around 75 ppm for C≡C. Assignment of the two alkyne carbons was possible from the

(28) (a) Cognacq, J. C.; Guillerme, G.; Chodkiewicz, W.; Cadiot, P. *Bull. Soc. Chim. Fr.* **1967**, *4*, 1190. (b) Madhavi, N. N. L.; Bilton, C.; Howard, J. A. K.; Allen, F. H.; Nangia, A.; Desiraju, G. R. *New J. Chem.* **2000**, *24*, 1.



analysis of the DEPT-135 spectra in which the quaternary carbons were nulled out. In the IR spectra, a weak $\nu(C\equiv C)$ absorption band is observed at ca. 2130 cm^{-1} , while strong absorptions assigned to $\nu(OH)$ and $\nu(\equiv CH)$ are evident at about 3550 and 3280 cm^{-1} , for **L₁** and **L₂**, respectively.

Synthesis and Characterization of the Mononuclear Allenylidene Complexes of Ruthenium(II) and Rhenium(I). The synthetic approach used to prepare the metal allenylidenes incorporating organic fragments derived from **L₁** and **L₂** was based on Selegue's protocol involving activation of the propargylic alcohols and intramolecular dehydration to give the allenylidene moieties.⁹ $[(triphos)Re(CO)_2(OTf)]$ (**1**) and $[RuCl(dppe)_2(OTf)]$ (**2**) were used as metal precursors in view of the well-known predisposition of both metal synthons to generate allenylidene complexes when reacted with propargylic alcohols [triphos = 1,1,1-tris(diphenylphosphinomethyl)ethane, dppe = 1,1-bis(diphenylphosphino)ethane].^{22,26} The use of the ruthenium triflate complex **2** instead of the corresponding dichloride allows for direct synthesis of the allenylidenes from the *cis/trans* isomeric mixture of $[RuCl_2(dppe)_2]$ without the need for recrystallization to obtain the *trans*- $[RuCl_2(dppe)_2]$ complex in pure form.²⁹ A similar approach was recently used for Ru complexes using the related BF_4 complex.²⁹ Complex **2** was straightforwardly generated by reaction of the dichloride complex with MeOTf in CH_2Cl_2 , giving MeCl as volatile byproduct, which is removed in vacuo in the workup.³⁰ Complex **2** is an air stable red-colored compound that is easily recrystallized from CH_2Cl_2/Et_2O mixtures.

Reactions of **1** with a slight excess of the alkynols **L₁** and **L₂** in CH_2Cl_2 at room temperature gave the corresponding mononuclear allenylidene complexes $[(triphos)Re(CO)_2\{C=C=C(\text{bianth})C(OH)(C\equiv CH)\}]OTf$ (bianth = bianthracenylidene) (**3**) and $[(triphos)Re(CO)_2\{C=C=C(\text{Ph})\{\mu-(p-C_6H_4)\}C(\text{Ph})(OH)(C\equiv CH)\}]OTf$ (**4**) (Scheme 1).³¹ The reactions were completed in 3–5 h, and the color of the solutions turned from yellow to deep purple, diagnostic of the formation of the polyunsaturated

cumulenyliene ligand.²⁶ By monitoring the reaction via $^{31}P\{^1H\}$ NMR spectroscopy no π -alkyne or hydroxyvinylidene intermediates were observed, which is however not surprising in rhenium allenylidene synthesis via the Selegue's reaction.^{26c,d,32}

The IR spectra of **3** and **4** show two $\nu(CO)$ bands in the range $2000\text{--}1920\text{ cm}^{-1}$, while no $\nu(C=C=C)$ band of the allenylidene ligand is visible, most likely because of overlapping with the more intense carbonyl stretching bands. The $^{31}P\{^1H\}$ NMR spectra consist of overlapping second-order AXX' spin systems centered at -17.12 ppm for **3** and -17.70 ppm for **4**. These results are in line with those reported for the known rhenium allenylidenes $[(triphos)(CO)_2Re\{C=C=C(R)Ph\}](OTf)$ ($R = H, Me, Ph$).^{26c,d}

Characteristic features of **3** and **4** in the $^{13}C\{^1H\}$ NMR spectra are the resonances of the allenylidene chain carbons, which appear at ca. 290 ($C\alpha$), 210 ($C\beta$), and 160 ppm ($C\gamma$), the first two signals as multiplets due to C–P coupling and the third as a singlet, and the signals of the free propargylic unit that are observed at ca. 86 ppm ($C\equiv CH$), 78 ppm ($C\equiv CH$), and 75 ppm ($C(OH)(C\equiv CH)$). In the 1H NMR spectra, the free $C\equiv CH$ alkyne proton appears at ca. 2.9 ppm as a singlet, while the OH signal is not observed, probably due to the overlapping with the CH_2 signals of the triphos ligand.

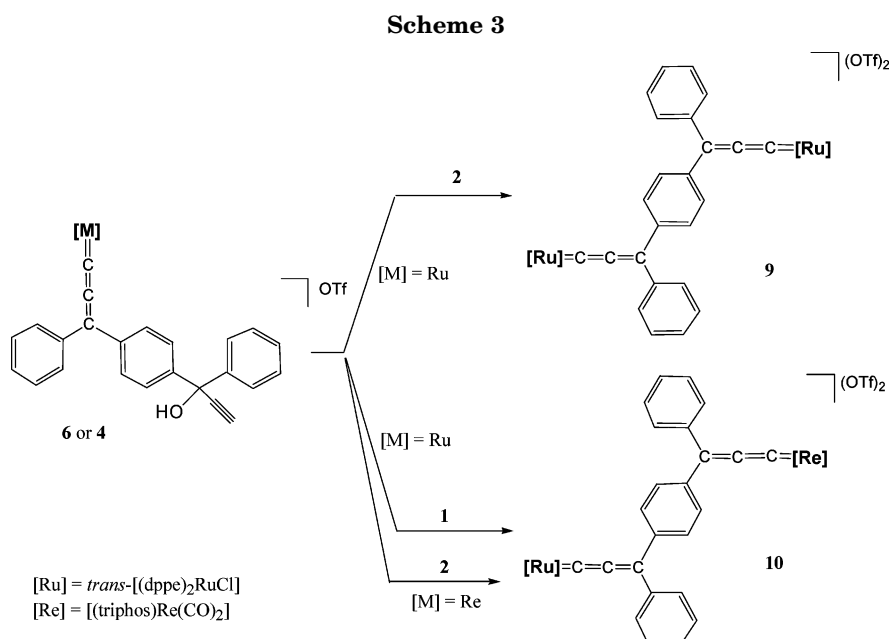
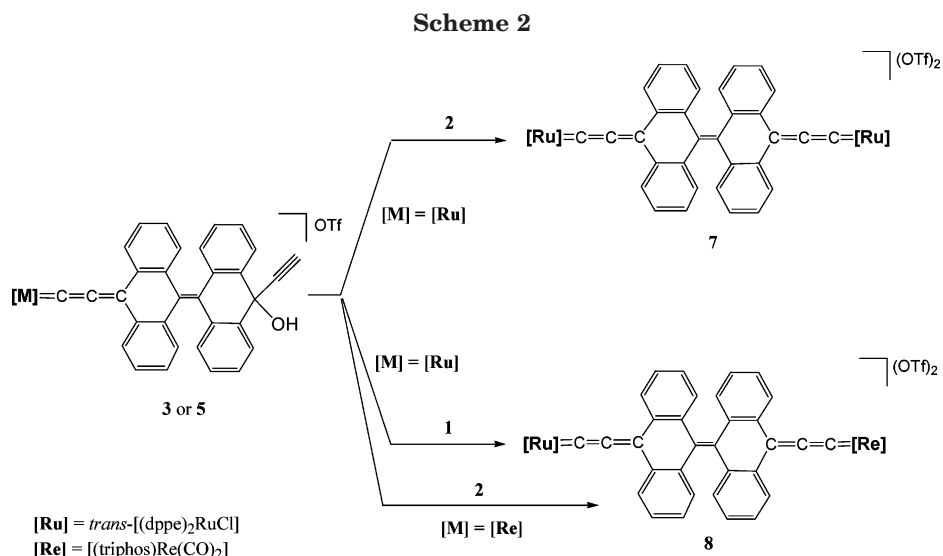
Under similar reaction conditions, the Ru(II) precursor **2** reacts with **L₁** and **L₂** to give the corresponding mononuclear allenylidenes *trans*- $[(dppe)_2RuCl\{C=C=C(\text{bianth})C(OH)(C\equiv CH)\}]OTf$ (**5**) and *trans*- $[(dppe)_2RuCl\{C=C=C(\text{Ph})\{\mu-(p-C_6H_4)\}C(\text{Ph})(OH)(C\equiv CH)\}]OTf$ (**6**) (Scheme 2). These reactions are slower than those observed for the rhenium precursor **1**, being completed in about 24 h, but also in this case no π -alkyne or hydroxyvinylidene intermediates were observed via NMR monitoring. The two novel ruthenium allenylidenes exhibit a common geometry corresponding to

(31) Reactions of **L₃** with either **1** and **2** to yield monometallic Re and Ru allenylidenes were successfully carried out in our laboratories. Further reactions to afford the corresponding bimetallic derivatives are still in progress, and the complete work will be described in detail in a future paper (manuscript in preparation).

(32) The formation of π -alkyne and hydroxyvinylidene species preceding the dehydration step in the Selegue's method is well documented for ruthenium complexes. See for example: Ciardi, C.; Reginato, G.; Gonsalvi, L.; de los Rios, I.; Romerosa, A.; Peruzzini, M. *Organometallics* **2004**, *23*, 2020, and references therein.

(29) Chin, B.; Luogh, A. J.; Morris, R. H.; Schweitzer, C. T.; D'Agostino, C. *Inorg. Chem.* **1994**, *33*, 6278.

(30) Bergamini, P.; Fabrizi De Biani, F.; Marvelli, L.; Mascellani, N.; Peruzzini, M.; Rossi, R.; Zanello, P. *New J. Chem.* **1999**, 207.



the *trans* disposition of chlorine and allenylidene ligands, as indicated in the $^{31}\text{P}\{^1\text{H}\}$ NMR spectra (CDCl_3) by the equivalence of the four phosphorus nuclei, with singlets at 38.07 and 38.48 ppm, respectively. The $^{13}\text{C}\{^1\text{H}\}$ NMR spectra of **5** and **6** show the α and β carbon atoms of the allenylidene unit as quintets at ca. 307 ppm ($J_{\text{CP}} \approx 14$ Hz) and 215 ppm ($J_{\text{CP}} \approx 3.5$ Hz), while the $\text{C}(\gamma)$ resonance appears at ca. 160 ppm as a singlet. The carbon atoms of the free propargylic moiety are evident as singlets at ca. 86, 77, and 75 ppm, attributed to $\text{C}\equiv\text{CH}$, $\text{C}\equiv\text{CH}$, and $\text{C}(\text{OH})(\text{C}\equiv\text{CH})$, respectively. The two latter assignments were supported by DEPT NMR experiments. In the IR spectra the strong $\nu(\text{C}=\text{C}=\text{C})$ absorption band is evident at 1917 cm^{-1} . Related allenylidene complexes of formula *trans*- $[(\text{dppe})_2\text{ClRu}\{\text{C}=\text{C}=\text{CR}^1\text{R}^2\}]\text{PF}_6$, synthesized by Dixneuf and co-workers, show similar spectroscopic data and therefore substantiate our assignment of *trans* geometry for **5** and **6**.^{22,33}

Synthesis and Characterization of Bimetallic Bis(allenylidene) Complexes. The mononuclear rhenium and ruthenium allenylidene complexes **3–6** bear a free propargylic group amenable to react with a second metal fragment to form bimetallic derivatives in which two metal allenylidene units can be held together by the organic spacer, either bianthracenylidene or phenylene. In contrast with expectations, the reaction of the monorhenium allenylidenes **3** and **4** with a second equivalent of **1** did not yield the homobimetallic Re/Re species. It was possible instead to obtain homobimetallic Ru/Ru and heterobimetallic Ru/Re bis(allenylidene) complexes starting from the Ru monoallenylidenes **5** and **6** (Schemes 2, 3) as expected. Thus, reaction of **5** with **1** and **2** afforded in fairly good yield the bis(allenylidene) complexes *trans,trans*- $[(\text{dppe})_2\text{Ru}(\text{Cl})\{\text{C}=\text{C}=\text{C}(\text{bianth})\text{C}=\text{C}=\text{C}\}(\text{Cl})\text{Ru}(\text{dppe})_2](\text{OTf})_2$ (**7**) and *trans*- $[(\text{dppe})_2\text{Ru}(\text{Cl})\{\text{C}=\text{C}=\text{C}(\text{bianth})\text{C}=\text{C}=\text{C}\}(\text{CO})_2\text{Re}(\text{triphos})](\text{OTf})_2$ (**8**) as deep violet microcrystalline materials. Similarly, treatment of **6** with the ruthenium and rhenium synthons **1** and **2** yielded *trans,trans*- $[(\text{dppe})_2\text{Ru}(\text{Cl})\{\text{C}=\text{C}=\text{C}(\text{Ph})\{\mu\text{-}(p\text{-C}_6\text{H}_4)\}(\text{Ph})\text{C}=\text{C}=\text{C}\}(\text{Cl})\text{Ru}(\text{dppe})_2](\text{OTf})_2$ (**9**) and *trans*- $[(\text{dppe})_2\text{Ru}(\text{Cl})\{\text{C}=\text{C}=\text{C}(\text{Ph})\{\mu\text{-}(p\text{-C}_6\text{H}_4)\}(\text{Ph})\text{C}=\text{C}=\text{C}\}(\text{CO})_2\text{Re}(\text{triphos})](\text{OTf})_2$ (**10**). Alternatively, the two heterobimetallic Ru/Re complexes **8**

(33) Touchard, D.; Pirio, N.; Dixneuf, P. H. *Organometallics* **1995**, *14*, 4920.

and **10** may be synthesized also by reacting the rhenium monoallenylidene **3** or **4** with the ruthenium precursor **2** under similar reaction conditions. A comparison of the NMR data of the isolated reaction products confirms that the heterobimetallic species **8** and **10** form irrespective of the monoallenylidene used as precursor.

The homonuclear diruthenium bis(allenylidenes) **7** and **9** are characterized in the ^{31}P NMR spectra by singlets at about 38 ppm as a consequence of the magnetic equivalence of the eight phosphorus atoms of the two $\text{Ru}(\text{dppe})_2$ units. In contrast, the heterobimetallic Ru/Re bis(allenylidenes) **8** and **10** show two set of signals ascribable to the $\text{Ru}(\text{dppe})_2$ and $\text{Re}(\text{triphos})$ cappings kept together by the bis(allenylidene) unit; the former appears as a singlet at ca. 38 ppm, while the latter exhibits the usual second-order AXX' multiplet at ca. -17 ppm.^{26c,d} The $^{13}\text{C}\{^1\text{H}\}$ NMR spectra **7** and **9** show a single set of resonances for the α , β , and γ carbon atoms in agreement with the equivalence of the two $\text{Ru}=\text{C}=\text{C}=\text{C}$ allenylidene ligands at ca. 310 ppm (quintet, J_{CP} 14 Hz), 230 (quintet, J_{CP} 3 Hz), and 160 (s) ppm, respectively.

In line with the proposed formulation, the heterobimetallic bis(allenylidene) compounds **8** and **10** allow discrimination of both the signals of $\text{Ru}=\text{C}=\text{C}=\text{C}$ and $\text{Re}=\text{C}=\text{C}=\text{C}$ units in their $^{13}\text{C}\{^1\text{H}\}$ NMR spectra. The $\text{C}(\alpha)$ and $\text{C}(\beta)$ signals can be unequivocally assigned on the basis of their multiplicity: $\text{C}(\alpha)$ and $\text{C}(\beta)$ of the $\text{Ru}=\text{C}=\text{C}=\text{C}$ unit appear as quintets at ca. 310 ppm ($J_{\text{CP}} \approx 14$ Hz) and 230 ppm ($J_{\text{CP}} \approx 3$ Hz), while the $\text{C}(\alpha)$ and $\text{C}(\beta)$ of the $\text{Re}=\text{C}=\text{C}=\text{C}$ unit appear as doublets of triplets at 290 ppm ($J_{\text{CPtrans}} \approx 22$ Hz, $J_{\text{CPcis}} \approx 8$ Hz) and 220 ppm ($J_{\text{CPtrans}} \approx 15$ Hz, $J_{\text{CPcis}} \approx 5$ Hz). The $\text{C}(\gamma)$ carbon atoms of both allenylidene units appear as singlets near 160 ppm (see Table 1). Further details about the NMR and IR characterization of all the mono- and bis(allenylidene) species are summarized in Table 1.

In the IR spectra **7** and **9** give a very strong $\nu(\text{C}=\text{C}=\text{C})$ band at 1917 cm^{-1} , while **8** and **10** have two strong $\nu(\text{CO})$ bands in the range $1920\text{--}2000\text{ cm}^{-1}$, likely overlapping with the $\nu(\text{C}=\text{C}=\text{C})$ stretching frequencies falling in the same region.

Electrochemical Properties of the Allenylidene Complexes. Complexes **7**, **8**, and **10** were studied using cyclic voltammetry in order to verify whether the homo- or heteroconjugated bis(allenylidene) moieties communicate electronic information between the two metal ends. The mononuclear allenylidenes **4**–**6** were also tested by electrochemical methods to compare how electronic effects act upon passing from a mononuclear allenylidene to a dinuclear bis(allenylidene) complex. As a representative example of these cooperative electronic effects, Figure 1 compares the cyclic voltammetric behavior of the monoruthenium complex *trans*-[(dppe) $_2$ - $\text{RuCl}\{\text{C}=\text{C}=\text{C}(\text{bianth})\text{C}(\text{OH})(\text{C}\equiv\text{CH})\}\text{OTf}$] (**5**) with that of the corresponding diruthenium complex *trans,trans*-[(dppe) $_2$ $\text{Ru}(\text{Cl})\{\text{C}=\text{C}=\text{C}(\text{bianth})\text{C}=\text{C}=\text{C}\}\{\text{Cl}\text{Ru}(\text{dppe})_2\}\text{OTf}$]₂ (**7**).

As in the case of the related monoallenylidene cation *trans*-[(dppe) $_2$ $\text{RuCl}\{\text{C}=\text{C}=\text{CPh}_2\}^+$ (**11**),¹⁴ complex **5** exhibits a well-defined reduction process showing partial chemical reversibility, which precedes a further irreversible reduction at the borders of the cathodic

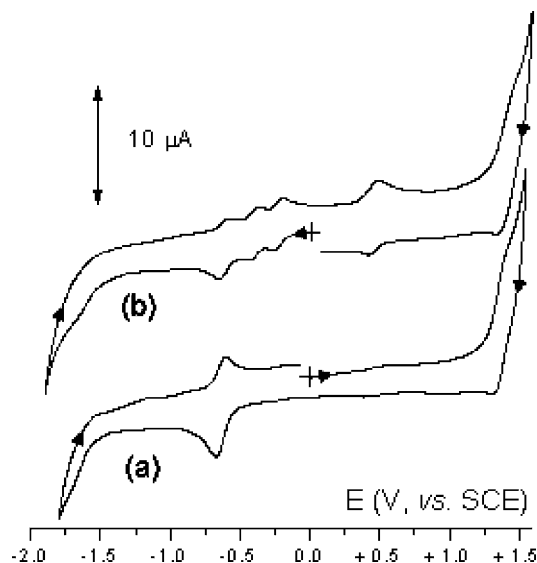


Figure 1. Cyclic voltammetric responses recorded at a platinum electrode in CH_2Cl_2 solution of (a) **5** (0.6×10^{-3} mol dm^{-3}); (b) **7** (0.5×10^{-3} mol dm^{-3}). $[\text{NBu}_4][\text{PF}_6]$ (0.2 mol dm^{-3}) supporting electrolyte. Scan rate 0.2 V s^{-1} .

window. An oxidation process is also present, whose chemical reversibility is only partially detectable because of the overlap with the solvent discharge. Noticeably, Osteryoung square wave voltammetry (OSQW) displays a peak-height similar to that of the reduction process.

Controlled potential coulometry corresponding to the first reduction carried out at low temperature ($-20\text{ }^\circ\text{C}$) consumed about one electron/molecule.³⁴ Hydrodynamic and cyclic voltammetric tests³⁵ on the reduced solution show profiles quite complementary to the original ones, thus confirming the chemical reversibility of the cathodic step.

Analysis of the cyclic voltammetric responses with scan rates varying from 0.02 to 2.00 V s^{-1} shows that the $i_{\text{pa}}/i_{\text{pc}}$ ratio, which is 0.55 at the lowest scan rate, increases only slightly to 0.64 at the highest scan rate. Even if such a finding would support the occurrence of side reactions accompanying the reduction process,³⁵ in view of the coulometric measurements, we are inclined to assign this effect to the above-mentioned fast reoxidation rather than to fragmentation processes.

When compared to **5**, the dinuclear complex **7** displays, in addition to the above-mentioned processes located at the extremities of the solvent window, a rather rich sequence of electron transfers, which appear to be chemically reversible in the cyclic voltammetric time scale. As shown in Figure 2, the cyclic voltammogram of **7** exhibits either a well-defined oxidation (peak system D/D') or two separated reductions (peak systems A/A' and B/B' , respectively), followed in turn by a further two times higher reductions (peak system C/C').

Step-by-step coulometric measurements corresponding to both the anodic process D and the two cathodic processes A and B proved their monoelectronic nature. Also in these cases hydrodynamic and cyclic voltam-

(34) Electrochemical tests at ambient temperature were discarded, as fast reoxidation triggered by traces of air continuously regenerates the original complex.

(35) Zanello, P. In *Inorganic Electrochemistry. Theory, Practice and Application*; RSC: Cambridge, UK, 2003.

Table 1. Selected ^1H , $^{31}\text{P}\{^1\text{H}\}$, and $^{13}\text{C}\{^1\text{H}\}$ NMR Spectral Data for Mono- and Bis(allenylidene) Complexes^a

Complex	^1H δ (ppm), J (Hz)	$^{31}\text{P}\{^1\text{H}\}$	$^{13}\text{C}\{^1\text{H}\}$ δ (ppm), J (Hz)		
		δ (ppm), J (Hz) IR (KBr, cm^{-1})			
<p style="text-align: center;">3^b</p>	1.67 (br s, 3H, $\text{CH}_{3\text{triphos}}$) 2.40 - 2.80 (m, 6H, $\text{CH}_{2\text{triphos}}$) 2.90 (s, 1H, $\text{C}\equiv\text{CH}$)	- 17.12 (m) v(OH) 3500-3100 br v($\equiv\text{CH}$) 3295 v($=\text{CH}_{\text{arom}}$) 3057 v(CO) 1998 v(CO) + v($\text{C}=\text{C}=\text{C}$) 1914 v($\text{C}=\text{C}$) 1590 v(OTf) 1275	290.0 (m, $\text{Re}=\text{C}=\text{C}=\text{C}$) 211.2 (s, $\text{Re}=\text{C}=\text{C}=\text{C}$) 195.0 (m, CO) 161.0 (m, $\text{Re}=\text{C}=\text{C}=\text{C}$) 145 - 150 (C_{arom}) 85.8 (s, $\text{C}\equiv\text{CH}$) 74.8 (s, $\text{C}\equiv\text{CH}$) 74.9 (s, $\text{C}(\text{OH})(\text{C}\equiv\text{CH})$) 40.0 (m, $\text{CH}_{3\text{triphos}}$ + $\text{CH}_3\text{C}_{\text{triphos}}$) 33 - 35 (br m, $\text{CH}_{2\text{triphos}}$)		
	<p style="text-align: center;">4^b</p>	1.72 (br s, 3H, $\text{CH}_{3\text{triphos}}$) 2.35 - 2.90 (br m, 6H, $\text{CH}_{2\text{triphos}}$) 2.96 (s, 1H, $\text{C}\equiv\text{CH}$)	- 17.70 (m) v(OH) 3500-3200 br v($\equiv\text{CH}$) 3288 v($=\text{CH}_{\text{arom}}$) 3057 v(CO) 1998 v(CO) + v($\text{C}=\text{C}=\text{C}$) 1917 v($\text{C}=\text{C}$) 1593, 1670 v(OTf) 1278	290.5 (m, $\text{Re}=\text{C}=\text{C}=\text{C}$) 209.6 (d, J_{CPtrans} 9.8, $\text{Re}=\text{C}=\text{C}=\text{C}$) 192.0 (m, CO), 161.4 (s, $\text{Re}=\text{C}=\text{C}=\text{C}$) 144 - 150 (C_{arom}) 85.8 (s, $\text{C}\equiv\text{CH}$) 77.9 (s, $\text{C}\equiv\text{CH}$) 74.9 (s, $\text{C}(\text{OH})(\text{C}\equiv\text{CH})$) 40.2 (q, J_{CP} 15.5, $\text{CH}_{3\text{triphos}}$) 40.1 (s, $\text{CH}_3\text{C}_{\text{triphos}}$) 33.0 - 34.8 (m, $\text{CH}_{2\text{triphos}}$)	
		<p style="text-align: center;">5^b</p>	2.60-3.30 (m, 8H, $\text{CH}_{2\text{dippe}}$) 2.97 (s, 1H, $\text{C}\equiv\text{CH}$)	38.07 (s) v(OH) + v($\text{C}\equiv\text{CH}$) 3600 - 3200 br v($=\text{CH}_{\text{arom}}$) 3057 v($\text{C}=\text{C}=\text{C}$) 1917 v($\text{C}=\text{C}$) 1589, 1575 v(OTf) 1272	307.4 (qu, J_{CP} 14.6, $\text{Ru}=\text{C}=\text{C}=\text{C}$) 216.0 (s, $\text{Ru}=\text{C}=\text{C}=\text{C}$) 159.6 (s, $\text{Ru}=\text{C}=\text{C}=\text{C}$) 149.5 - 143.3 (C_{arom}) 85.8 (s, $\text{C}\equiv\text{CH}$) 76.3 (s, $\text{C}\equiv\text{CH}$) 75.2 (s, $\text{C}(\text{OH})(\text{C}\equiv\text{CH})$) 26.9 (qu, J_{CP} 12.2, $\text{CH}_{2\text{dippe}}$)

Table 1 (Continued)

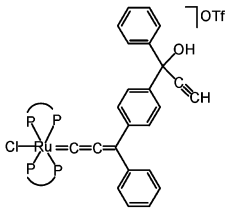
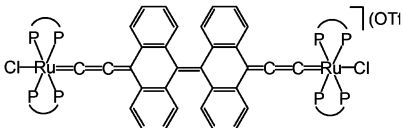
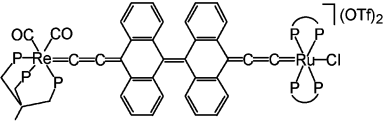
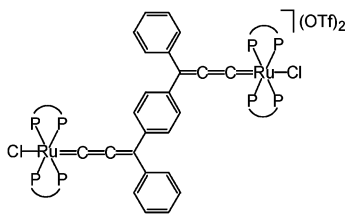
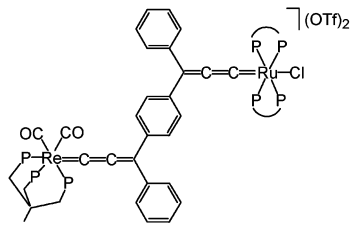
Complex	^1H δ (ppm), J (Hz)	$^{31}\text{P}\{^1\text{H}\}$	$^{13}\text{C}\{^1\text{H}\}$ δ (ppm), J (Hz)
		δ (ppm), J (Hz) IR (KBr, cm^{-1})	
 <p style="text-align: center;">6^b</p>	2.50 - 2.90 (m, 8H, CH_2 _{dpppe}) 2.96 (s, 1H, $\text{C}\equiv\text{CH}$)	38.48 (s) v(OH) 3600-3200br v($\equiv\text{CH}$) 3293 v($=\text{CH}_{\text{arom}}$) 3052 v($\text{C}=\text{C}=\text{C}$) 1917 v($\text{C}=\text{C}$) 1589 v(OTf) 1278	307.6 (qu, J_{CP} 14.0, $\text{Ru}=\text{C}=\text{C}=\text{C}$) 215.6 (qu, J_{CP} 3.5, $\text{Ru}=\text{C}=\text{C}=\text{C}$) 160.8 (s, $\text{Ru}=\text{C}=\text{C}=\text{C}$) 149.6 - 144.2 (C_{arom}) 85.8 (s, $\text{C}\equiv\text{CH}$) 77.9 (s, $\text{C}\equiv\text{CH}$) 74.6 (s, $\text{C}(\text{OH})(\text{C}=\text{CH})$) 28.1 (qu, J_{CP} 11.0, CH_2 _{dpppe})
 <p style="text-align: center;">7</p>	2.38 - 2.95 (m, 16H, CH_2 _{dpppe})	38.12 (s) v(CH_{arom}) 3053 v($\text{C}=\text{C}=\text{C}$) 1917 v($\text{C}=\text{C}$) 1589, 1670 v(OTf) 1269	11.3 (qu, J_{CP} 14.0, $\text{Ru}=\text{C}=\text{C}=\text{C}$) 229.1 (qu, J_{CP} 3.0, $\text{Ru}=\text{C}=\text{C}=\text{C}$) 158.5 (s, $\text{Ru}=\text{C}=\text{C}=\text{C}$) 135.1-126.7 (C_{arom}) 28.2 (qu, J_{CP} 11.6, CH_2 _{dpppe})
 <p style="text-align: center;">8</p>	1.80 (q, 3H, J_{CP} 9.6 CH_3 _{triphos}) 2.25 - 2.90 (br m, 14H, CH_2 _{triphos} + CH_2 _{dpppe})	37.52 (s, dppe) -18.59 (m, triphos)	310.9 (qu, J_{CP} 12.8, $\text{Ru}=\text{C}=\text{C}=\text{C}$) 284.0 (dt, J_{CPtrans} 20.1, J_{CPcis} 8.5, $\text{Re}=\text{C}=\text{C}=\text{C}$) 227.9 (qu, J_{CP} 2.0, $\text{Ru}=\text{C}=\text{C}=\text{C}$) 206.8 (dt, J_{CPtrans} 12.8, J_{CPcis} 5.0, $\text{Re}=\text{C}=\text{C}=\text{C}$) 192.0 (m, CO) 159.1, 159.5 (all s, $\text{Ru}=\text{C}=\text{C}=\text{C}$ + $\text{Re}=\text{C}=\text{C}=\text{C}$) 144.5 - 125.3 (C_{arom}) 40.1 (br, $\text{CH}_3\text{C}_{\text{triphos}}$) 39.9 (q, J_{CP} 9.6, CH_3 _{triphos}) 33.5 (m, $\text{CH}_2\text{P}_{\text{ax}}$ _{triphos}) 34.7 - 30.7 (br m, $\text{CH}_2\text{P}_{\text{eq}}$ _{triphos}) 28.2 (qu, J_{CP} 11.6, CH_2 _{dpppe})

Table 1 (Continued)

Complex	^1H δ (ppm), J (Hz)	$^{31}\text{P}\{^1\text{H}\}$ δ (ppm), J (Hz) IR (KBr, cm^{-1})	$^{13}\text{C}\{^1\text{H}\}$ δ (ppm), J (Hz)
 <p style="text-align: center;">9</p>	2.25 – 2.85 (m, 16H, $\text{CH}_{2\text{dpppe}}$)	38.10 (s) v(CH_{arom}) 3050 v($\text{C}=\text{C}=\text{C}$) 1916 v($\text{C}=\text{C}$) 1583, 1578 v(OTf) 1276	307.9 (qu, J_{CP} 14.0, Ru=C=C=C) 229.1 (qu, J_{CP} 3.0, Ru=C=C=C) 160.8 (s, Ru=C=C=C) 135.7-126.5 (C_{arom}) 28.1 (qu, J_{CP} 11.2, $\text{CH}_{2\text{dpppe}}$)
 <p style="text-align: center;">10</p>	1.76 (br s, 3H, $\text{CH}_{3\text{triphos}}$) 2.20 – 3.00 (br m, 14H, $\text{CH}_{2\text{triphos}}$ + $\text{CH}_{2\text{dpppe}}$)	37.71 (s, dppe) - 18.28 (m, triphos) v(CH_{arom}) 3063 v(CO + C=C=C) 1998, 1913 v(C=C) 1588, 1579 v(OTf) 1273	311.2 (qu, J_{CP} 13.9, Ru=C=C=C) 292.4 (dt, $J_{\text{C}^{\text{trans}}}$ 22.0, $J_{\text{C}^{\text{cis}}}$) 8.2, Re=C=C=C) 227.7 (qu, J_{CP} 2.8, Ru=C=C=C) 218.5 (dt, $J_{\text{C}^{\text{trans}}}$ 15.5, $J_{\text{C}^{\text{cis}}}$ 4.7, Re=C=C=C) 191.9 (m, CO) 161.0, 159.5 (all s, Ru=C=C=C + Re=C=C=C) 138.0-127.2 (C_{arom}) 40.1 (q, J_{CP} 2.5, $\text{CH}_3\text{C}_{\text{triphos}}$) 39.7 (q, J_{CP} 7.8, $\text{CH}_{2\text{triphos}}$) 35.6 (dt, $J_{\text{CP ax}}$ 14.6, $J_{\text{CP eq}}$ 2.4, $\text{CH}_2\text{P}_{\text{ax triphos}}$) 34.4 (br m, $\text{CH}_2\text{-P}_{\text{eq triphos}}$) 28.1 (qu, J_{CP} 11.3, $\text{CH}_{2\text{dpppe}}$)

^a All the NMR spectra were recorded in CDCl_3 , at room temperature (20 °C) on a Bruker AC200 instrument. Key: d, doublet; t, triplet; q, quartet; qu, quintet; m, multiplet; br, broad. ^b OH proton not observed.

metric tests on the resulting solutions confirmed the chemical reversibility of the processes even in the long times required for macroelectrolysis. In contrast, the subsequent exhaustive two-electron reduction corresponding to peak C revealed partial degradation of the original complex.

Tables 2 and 3 summarize the values of formal electrode potentials for the electron transfer processes of complexes **5** and **7**, together with those of the other mono- and bis(allylidyne) complexes investigated by electrochemical methods.

A few data taken from the literature for other related complexes are also reported in the tables for comparative purposes. For example, the related bis(allylidyne)diruthenium(II) complexes $[\text{Cl}(\text{dppe})_2\text{Ru}\{\text{C}=\text{C}=\text{C}(\text{H})\text{-X-(H)C}=\text{C}=\text{C}\}\text{Ru}(\text{dppe})_2\text{Cl}]^{2+}$ (X = 1,4- C_6H_4 , **12**; 2,5- $\text{C}_4\text{H}_2\text{S}$, **13**) show two sequential, reversible, one-electron reductions.¹² Although the redox pattern observed was more complicated, it was proposed that in

ruthenium-allylidenes the reduction processes are centered on the unsaturated ligand,^{14,16,17} whereas the oxidation processes are centered on the ruthenium atom.^{15,16} Thus, we assign by comparison the peak system D/D' to the Ru(II)/Ru(III) oxidation of one metal center, whereas the oxidation of the other Ru(II) center is likely to be masked by the solvent discharge. The mononuclear allylidenes **6** and **4** and the heterodinuclear complexes **8** and **10** exhibit voltammetric patterns substantially similar to those described above for the couple **5** and **7**, the only significant difference being that in **10** the anodic process is markedly shifted toward positive potential values.

In summary, from the analysis of the electrochemical data it is evident that the splitting of the cumulene-centered reduction(s) on passing from mononuclear allylidenes to dinuclear bis(allylidenes) is not affected by the bianthracenyli-dene spacer, which therefore does not inhibit the electronic communication

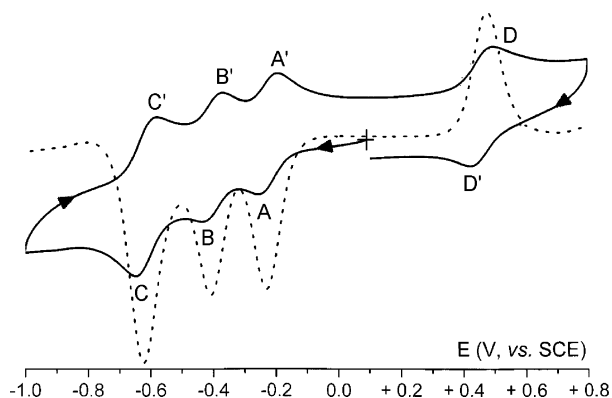


Figure 2. Cyclic (—) and Osteryoung square wave (---) voltammetric responses recorded at a platinum electrode in CH_2Cl_2 solution of **7** ($0.5 \times 10^{-3} \text{ mol dm}^{-3}$). $[\text{NBu}_4][\text{PF}_6]$ (0.2 mol dm^{-3}) supporting electrolyte. Scan rates: (—) 0.2 V s^{-1} ; (---) 0.1 V s^{-1} .

Table 2. Formal Electrode Potentials (V, vs SCE) and Peak-to-Peak Separations (mV) for the Electron Transfer Processes Exhibited by the Mononuclear Ru(II) and Re(I) Allenylidenes in CH_2Cl_2 Solution

complex	oxidation process		reduction processes			ref
	$E^\circ(2+/+)$	ΔE_p^a	$E^\circ(+/0)$	ΔE_p^a	$E^\circ(0/-)$	
4	+1.30	76	-0.46	74	-1.5 ^b	c
5	+1.36 ^{d,e}		-0.60	60	-1.6 ^b	c
6	+1.40 ^{d,e}		-0.61	61	-1.7 ^b	c
11			-0.64	60	-1.72 ^b	14

^a Measured at 0.1 V s^{-1} . ^b Peak potential value for irreversible processes. ^c Present work. ^d Potential value measured by OSQW. ^e Peak height measured by OSQW.

between the two Ru=C=C=C fragments. The separation of 0.19 V for the sequence $2+/+/0$ for **7**, **8**, and **10** gives a K_{com} value of 1.6×10^3 , which suggests that the positive charge is partially delocalized along the allenylidene chain in the singly reduced species.³⁵ The eventual interaction between the two metal centers is more difficult to assess, as the second oxidation is partially overlapped by the solvent discharge. At any scan rate a value for K_{com} of **7** was roughly estimated on the order of 10^{16} , which suggests that the further positive charge generated at the first oxidation is completely delocalized between the two ruthenium centers (Robin-Day Class III mixed-valent $\text{Ru}^{\text{II}}\text{Ru}^{\text{III}}$ species).³⁵ The unambiguous assignment of the two-electron process C/C' is also problematic, as it could be due either to the concomitant Ru(II)/Ru(I) reduction of the two Ru(II) centers or to the further reduction of the unsaturated chain.³⁶

UV-Vis and EPR Spectral Characterizations of the Redox Processes of Allenylidene Complexes. The UV-vis spectra recorded in an optically transparent

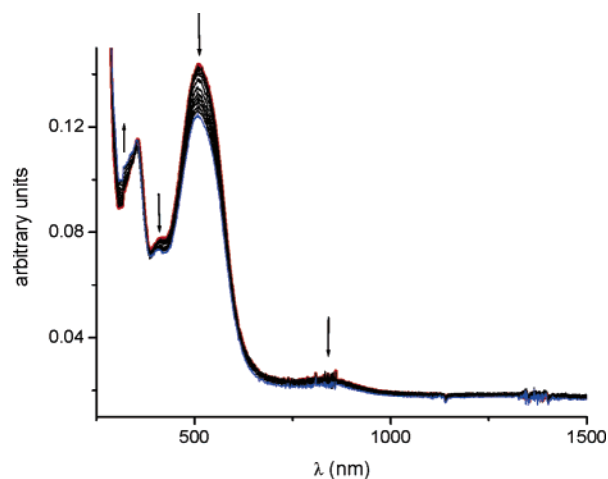


Figure 3. UV-vis spectra recorded in an optically transparent thin-layer electrode (OTTLE) cell during the stepwise reduction of complex **5** in CH_2Cl_2 solution.

thin-layer electrode (OTTLE) cell during the stepwise reduction of complex **5** in CH_2Cl_2 solution are illustrated in Figure 3, showing (arrows) two intense absorptions at $\lambda_{\text{max}} = 504$ and 358 nm , respectively, and a weak band at $\lambda_{\text{max}} = 850 \text{ nm}$. Two further shoulders are present at 325 and 412 nm , respectively.

According to DFT calculations on model $[(\text{CO})_5\text{M}(\text{=C})_n\text{H}_2]$ ($n = 2, 9$) complexes,³⁷ the two low-energy bands are assigned to the geometrically permitted LUMO \leftarrow HOMO-1 transition ($\lambda_{\text{max}} = 504 \text{ nm}$) and to the geometrically forbidden weak LUMO \leftarrow HOMO transition ($\lambda_{\text{max}} = 850 \text{ nm}$), respectively. On the basis of the electrochemical results and on earlier theoretical calculations, the LUMO \leftarrow HOMO transition could be described as a MLCT from a $d\pi$ metal orbital to π^* orbital of the ligand.³⁸ Both transitions display a bathochromic shift with respect to the related Ru(II) cumulenes $[\text{Cl}(\text{PR}_3)_4\text{Ru}(\text{=C})_n\text{R}_2]^+$, where the weak peak is detected around 600 nm , while the main absorption band is around 400 nm .^{15,16,38} Such a shift is likely due to the presence of the aromatic terminal groups in **5**, which strengthen the cumulene conjugation responsible for the red shift.³⁸ The shoulder present at $\lambda = 412 \text{ nm}$, near the LUMO \leftarrow HOMO-1 band, is a spin-forbidden singlet-triplet transition. The two intense peaks present in the high-energy region ($\lambda_{\text{max}} = 270$ and 212 nm , respectively) are typical of n/π^* and π/π^* transitions of the phosphine groups.¹⁵ As far as the corresponding dinuclear complex **7** is concerned, it displays a spectral pattern qualitatively similar to that of **5**, except for the main absorption, which is shifted to $\lambda_{\text{max}} = 545 \text{ nm}$ (Figure 4). The shift is due to the delocalization of the LUMO on a longer conjugated carbon chain, whose stabilizing effect decreases the LUMO \leftarrow HOMO-1

Table 3. Formal Electrode Potentials (V, vs SCE) and Peak-to-Peak Separations (mV) for the Most Significant Electron Transfer Processes Exhibited by the Dinuclear Ru/Ru and Ru/Re Allenylidenes in CH_2Cl_2 Solution

complex	$E^\circ(3+/2+)$	ΔE_p^a	$E^\circ(2+/+)$	ΔE_p^a	$E^\circ(+/0)$	ΔE_p^a	$E^\circ(0/2-)$	ΔE_p^a
7	+0.46	59	-0.22	59	-0.41	59	-0.62	57
8	+0.47	59	-0.15	76	-0.34 ^b		-0.44 ^b	
10	+1.07 ^b		-0.16	58	-0.35 ^b		-0.64 ^b	
12			-0.08 ^c	66 ^c	-0.28 ^c	81 ^c		
13			+0.10 ^c	71 ^c	-0.18 ^c	80 ^c		

^a Measured at 0.1 V s^{-1} . ^b Measured by OSWV. ^c From ref 12.

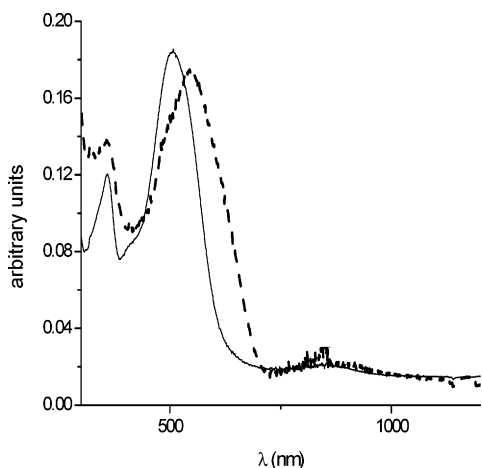


Figure 4. UV/vis spectra of **5** (—) and **7** (---) in CH_2Cl_2 solution.

Table 4. λ_{max} for the LUMO \leftarrow HOMO and LUMO \leftarrow HOMO-1 Bands of Complexes 4-8 and 10

compound	λ_{max} (nm)	
	LUMO \leftarrow HOMO	LUMO \leftarrow HOMO-1 ^a
4	865	504*, 550
5	850	504
6	860	524
7	856	504*, 545
8	852	502*, 552
10	862	502*, 552

^a * = Shoulder.

gap.^{36,37} Furthermore, partial overlapping of a few bands is indicated by the broadness of the band at $\lambda_{\text{max}} = 545$ nm. The wavelengths for the most significant electronic transitions of all complexes are listed in Table 4.

To confirm the cumulene-centered nature of the first reduction of **7**, EPR measurements were carried out on the solution resulting from exhaustive one-electron reduction at 253 K. Figure 5 shows the main X-band EPR spectra.

Under glassy conditions ($T = 100$ K), the line shape analysis is suitably carried out in terms of the $S = 1/2$ anisotropic Hamiltonian resolved in rhombic structure.³⁹ The three broad signals are well separated and centered at g_i values typical of a paramagnetic species with the unpaired electron basically centered on the ligand framework, even if in the presence of some metallic character (rhombic symmetry, $g_i \neq g_{\text{electron}} = 2.0023$). In particular, the multiple derivative analysis strongly supports that the electron spin density is localized inside the C=C chain, as there is no evidence for any ³¹P satellite splittings. In the limits of the experimental anisotropic ΔH_i line widths [$a_i(^{99,103}\text{Ru}) \leq \Delta H_i$, $g_i = 2.047(5)$; $g_m = 2.023(5)$; $g_h = 2.002(5)$; $\langle g \rangle = 2.024(5)$. $\Delta H_l = 16(1)$ G, $\Delta H_m = 16(1)$ G, $\Delta H_h = 14(1)$ G]⁴⁰ no hyperfine (hpf) splittings due to Ru isotopes are detectable.

(36) Skibar, W.; Kopacka, H.; Wurst, K.; Salzmann, C.; Ongania, K.-H.; Fabrizi de Biani, F.; Zanello, P.; Bildstein, B. *Organometallics* **2004**, *23*, 1024.

(37) Re, N.; Sgamellotti, A.; Floriani, C. *Organometallics* **2000**, *19*, 1115.

(38) Slageren, J.; Winter, R. F.; Klein, A.; Hartmann, S. *J. Organomet. Chem.* **2003**, *670*, 137.

(39) (a) Pilbrow, J. H. *Transition Ion Electron Paramagnetic Resonance*; Clarendon Press: Oxford, 1990. (b) Mabbs, F. E.; Collison, D. *Electron Paramagnetic Resonance of d Transition Metal Compounds*, Vol. 16 of *Studies in Inorganic Chemistry*; Elsevier: New York, 1992.

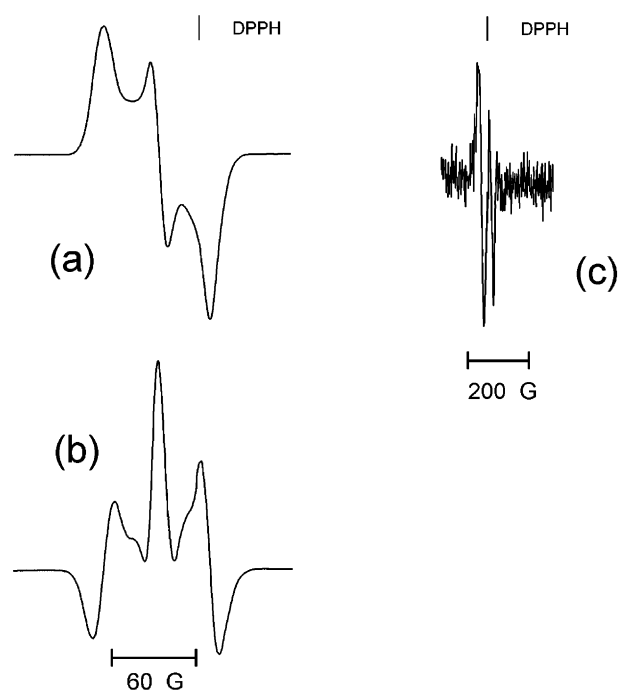


Figure 5. (a, b) First and second derivative spectra of the exhaustively one-electron-reduced CH_2Cl_2 solution of **7**; (c) first derivative spectrum of the solution at room temperature.

Raising the temperature to the glassy-fluid transition ($T = 176$ K) the anisotropic line shape collapses in the corresponding isotropic signal. As shown in Figure 5c, in fluid solution ($T = 293$ K) the reduced complex displays two narrow signals, the low-field one being the isotropic one ($g_{\text{isotropic}} = 2.023(8)$; $\Delta H_{\text{isotropic}} = 12(6)$ G). Multiple derivative analysis does not evidenciate satellite metal or ligand hpf and shpf signals. The $\langle g \rangle$ and $g_{\text{isotropic}}$ features are in perfect agreement, confirming that the reduced complex maintains the primary geometry under different experimental conditions.

Upon progressive one-electron reduction of **7**, as illustrated in Figure 6, the LUMO \leftarrow HOMO transition band increases markedly and a new band at $\lambda_{\text{max}} = 1361$ nm appears, which corresponds to the formation of a mixed valence compound.

The one-electron reduction of complex **7** generates a completely delocalized Robin-Day Class III mixed valent species, as evidenced by the value $\Delta\nu_{1/2(\text{experimental})}$ of 1232 cm^{-1} against $\Delta\nu_{1/2(\text{theoretical})}$ of 4114 cm^{-1} predicted for an intervalence band of Robin-Day Class II symmetric complexes.⁴¹

As a general trend, all the mononuclear complexes exhibit upon one-electron reduction a progressive decrease of the bands associated with the LUMO \leftarrow HOMO-1 and LUMO \leftarrow HOMO transitions. In contrast, in the binuclear compounds the former band decreases, whereas the latter increases. In addition, as happens for complex **7**, all the binuclear complexes display a broad band at $\lambda_{\text{max}} \approx 500$ nm (LUMO \leftarrow HOMO-1 transition), which results from the presence of overlapping peaks.

(40) Lozos, J. P.; Hoffman, B. M.; Franz, C. G. *QCPE* **1974**, *11*, 265.

(41) (a) Hush, N. S. In *Progress in Inorganic Chemistry*; Cotton, F. A., Ed.; J. Wiley and Sons: New York, 1967; Vol. 8, p 391. (b) Dowling, N.; Henry, P. M.; Lewis, N. A.; Taube, H. *Inorg. Chem.* **1981**, *20*, 2345.

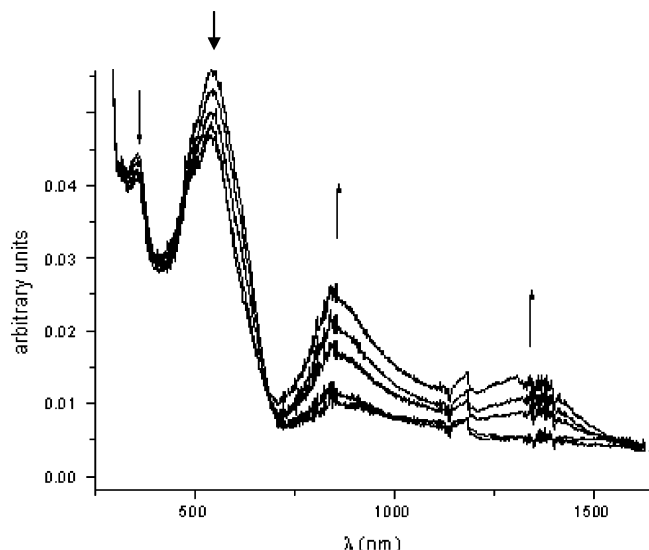


Figure 6. UV/vis spectra recorded in an OTTLE cell upon stepwise reduction of **7** in CH_2Cl_2 solution.

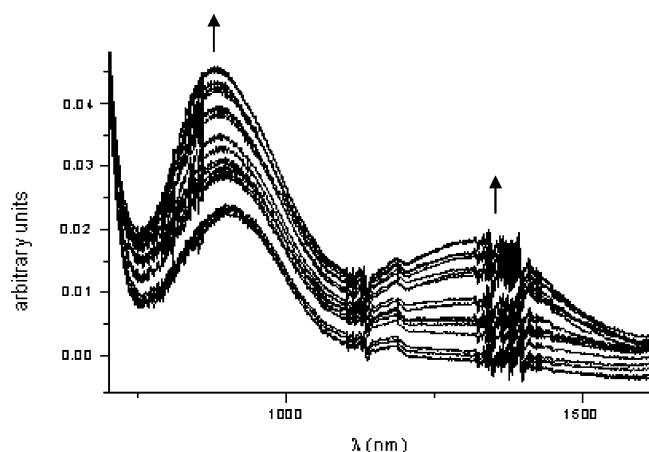


Figure 7. UV/vis spectra recorded in an OTTLE cell upon stepwise oxidation of **7** in CH_2Cl_2 solution.

The CT band diagnostic for the formation of mixed valence species as a consequence of the first reduction was detected for complex **10** (in the range 1120–1411 nm), although we were unable to reveal it for complex **8**. In the case of homodinuclear complex **7**, the one-electron oxidation product did not reveal detectable EPR signals. The spectroelectrochemical trend shown in Figure 7 matches essentially that illustrated in Figure 6 relative to the reduction process, but for a weaker change of the LUMO ← HOMO–1 transition band.

Upon progressive oxidation, a new charge transfer band appears at 1327 nm, which suggests the formation of a mixed valence species. As in the case of the reduction process, the experimental bandwidth ($\Delta\nu_{1/2} = 1972 \text{ cm}^{-1}$) strongly differs from the theoretical value expected for a Class II Robin-Day complex ($\Delta\nu_{1/2} = 4166 \text{ cm}^{-1}$), thus suggesting that, in agreement with the electrochemical findings, the oxidation leads to a completely delocalized Robin-Day Class III trication.

Conclusions

In summary, novel mono- and bis(allynylidenes) of Ru and Re bridged by multiconjugated aromatic organic spacers were obtained and their electrochemical and

spectroelectrochemical properties were measured in detail. Both techniques highlighted the presence of electronic communication between the metal centers through the multiconjugated organic chains; in particular the bianthracenylidene spacer brings about cumulene-centered reversible reductions, which are not interrupted on passing from mononuclear allynylidenes to dinuclear bis(allynylidenes), accompanied by an increase of LUMO ← HOMO transition band corresponding to the formation of a completely delocalized Robin-Day Class III mixed valent tricationic species.

Experimental Section

General Procedures. All reactions and manipulations were routinely performed under a dry nitrogen atmosphere by using standard Schlenk-tube techniques. Tetrahydrofuran (THF) was freshly distilled over LiAlH_4 ; *n*-hexane was stored over molecular sieves and purged with nitrogen prior to use; dichloromethane and methanol were purified by distillation over CaH_2 before use. The diketones, [9,9']bianthracenylidene-10,10'-dione and (4-benzoylphenyl)phenylmethanone, were purchased from Aldrich and used without further purification. The starting complexes [(tripos)(CO) $_2$ Re(OTf)] (**1**)³⁰ and $[\text{RuCl}_2(\text{dppe})_2]$ (*cis* + *trans*)⁴² were prepared as reported in the literature. All the other reagents and chemicals were commercial products and, unless otherwise stated, were used as received without further purification.

The solid complexes were collected on sintered glass frits and washed with either diethyl ether or *n*-hexane before being dried in a stream of nitrogen unless otherwise stated. IR spectra were obtained as KBr pellets using a Nicolet 510P FT-IR (4000–200 cm^{-1}) spectrophotometer. UV–visible spectra were carried out by use of a Perkin-Elmer LAMBQ 40 UV/vis spectrophotometer in CH_2Cl_2 using silica quartz cells (0.2 cm path length). Deuterated solvents for NMR measurements (Aldrich) were predried over molecular sieves (4 Å). ^1H and $^{13}\text{C}\{^1\text{H}\}$ NMR spectra were recorded at room temperature in degassed CDCl_3 on a Bruker AC200 spectrometer operating at 200.13 MHz (^1H) and 50.32 (^{13}C), respectively. Peak positions are relative to tetramethylsilane and were calibrated against the residual solvent resonance (^1H) or the deuterated CDCl_3 solvent multiplet (^{13}C). $^{31}\text{P}\{^1\text{H}\}$ NMR spectra (CDCl_3) were recorded on the same instrument operating at 81.01 MHz. Chemical shifts were measured relative to external 85% H_3PO_4 with downfield values taken as positive. $^{13}\text{C}\{^1\text{H}\}$ DEPT-135 NMR experiments were run on the Varian VXR300 spectrometer. Selected NMR and IR data for the mono- and bis(allynylidene) complexes are given in Table 1. Mass spectra (EI) were obtained at a 70 eV ionization potential and are reported in the form m^+/z (intensity relative to base = 100). Elemental analyses (C, H, N, S) were performed at the University of Ferrara using a Carlo Erba model 1106 elemental analyzer. Materials and apparatus for electrochemistry, spectroelectrochemistry, and EPR spectroscopy have been described elsewhere.^{44,45} All the potential values are referenced to the saturated calomel electrode (SCE). Under the present experimental conditions, the one-electron oxidation of ferrocene occurs at $E^\circ = +0.39 \text{ V}$.

Synthesis of Alkynol Precursors. The appropriate diketone (10 mmol) was dissolved in THF (50 mL) under a nitrogen

(42) Chaudret, B.; Commenges, G.; Poilblanc, R. *J. Chem. Soc., Dalton Trans.* **1984**, 1635.

(43) Chin, B.; Lough, A. J.; Morris, R. H.; Schweitzer, C. T.; D'Agostina, C. *Inorg. Chem.* **1994**, *33*, 6278.

(44) Fabrizi de Biani, F.; Corsini, M.; Zanello, P.; Yao, H.; Bluhm, M. E.; Grimes, R. N. *J. Am. Chem. Soc.* **2004**, *126*, 11360.

(45) Ciani, G.; Sironi, A.; Martinengo, S.; Garlaschelli, L.; Della Pergola, R.; Zanello, P.; Laschi, F.; Masciocchi, N. *Inorg. Chem.* **2001**, *40*, 3905.

atmosphere. Ethynylmagnesium chloride (4 equiv, 0.5 M in THF) was then slowly added under stirring within 12 h at room temperature with formation of a pale yellow precipitate. The reaction could be monitored by TLC (eluent: petroleum ether/ethyl acetate, 5:1). After cooling to 0 °C and dilution with diethyl ether (100 mL) the reaction mixture was hydrolyzed with a NH₄Cl-saturated aqueous solution (100 mL) and extracted three times with diethyl ether (50 mL each). The organic phase was washed with brine and dried over Na₂SO₄. The solvent was evaporated and the residue extracted with CH₂Cl₂, which was finally removed in vacuo to afford the final compound.

10,10'-Diethynyl-10H,10'H-[9,9']bianthracenylidenene-10,10'-diol. [9,9']Bianthracenylidenene-10,10'-dione (1.92 g, 5.0 mmol) was reacted with ethynylmagnesium chloride (40 mL, 0.5 M THF solution, 20 mmol) in THF (30 mL) to afford, after workup as described above, 2.03 g of compound **L**₁ [**L**₁ = (HC≡C)(OH)C(bianth)C(OH)(C≡CH)] as a yellow solid. Yield: 93%. Anal. Found: C, 88.16; H, 4.28. C₃₂H₂₀O₂ requires: C, 88.05; H, 4.62. IR (KBr, ν/cm⁻¹): 3391 (br, OH), 3283 (≡CH), 3061 (C≡C). ¹H NMR (200 MHz, CDCl₃): δ 7.63–7.57 (m, 8H, CH arom); 7.34–7.26 (m, 8H, CH arom); 2.92 (2H, br s, OH); 2.86 (s, 2H, CH). ¹³C{¹H} NMR (50.23 MHz, CDCl₃): δ 144.11, 143.98 (C_q arom); 128.27; 127.87; 125.94; 125.91 (CH arom); 86.25 (C_q); 75.64 (≡CH); 74.05 (C≡CH); 67.83 (s, C_{quat} C(OH)C). GC/MS *m/z*: 436(22); 402(100).

1-[4-(1-Hydroxy-1-phenylprop-2-ynyl)phenyl]-1-phenylprop-2-yn-1-ol. (4-Benzoylphenyl)phenyl methanone (2.86 g) was reacted with ethynylmagnesium chloride as described above to afford 3.21 g of compound **L**₂ [**L**₂ = (HC≡C)(HO)(Ph)C{μ-(*p*-C₆H₄)}C(Ph)(OH)(C≡CH)] as a pale yellow solid. Yield: 95%. Anal. Found: C, 85.91; H, 5.24. C₂₄H₁₈O₂ requires: C, 85.18; H, 5.36. IR (KBr, ν/cm⁻¹): 3554 (br OH), 3288 (≡CH), 3052 (CH arom), 2115 (C≡C). ¹H NMR (200 MHz, CDCl₃): δ 7.57–7.63 (m, 7H, arom); 7.27–7.38 (m, 7H arom); 3.04 (bs, 2H, OH); 2.85 (s, 2H, ≡C–H). ¹³C{¹H} NMR (50.23 MHz, CDCl₃): δ 143.99 (s, C_q, arom), 125.91–128.27 (all s, CH, arom), 86.26 (s, C≡CH), 75.52 (s, C≡CH), 74.07 (s, C_q, C(OH)C). GC/MS *m/z*: 314(16).

Synthesis of [RuCl(dppe)₂](OTf) (2). A mixture of [RuCl₂(dppe)₂] (*cis* + *trans*) (100 mg, 0.103 mmol) in dichloromethane (10 mL) was treated with CH₃OTf (29.5 μL, 0.258 mmol) and stirred at room temperature for 2 h. The color changed from yellow to red. The solution was concentrated to ca. 2 mL and, by slow addition of diethyl ether, an orange-brown solid precipitated. Yield: 90%. Anal. Found: C, 58.1; H, 4.20; S, 2.63. C₅₃H₄₈P₄RuClF₃SO₃ requires: C, 58.7; H, 4.43; S, 2.95. IR (KBr, ν/cm⁻¹): 1284 (OTf).^{19b} The NMR characterization of the complex cation of **2** is in line with the data reported⁴³ for the PF₆ and BF₄ analogues. ³¹P{¹H} NMR (81.01 MHz, CD₂-Cl₂): δ 83.67 (t), 56.21 (t), *J*_{PP} 12.7 Hz.

Synthesis of Mono- and Bis(allenylidene) Complexes. [(triphos)Re(CO)₂{C=C=C(bianth)C(OH)(C≡CH)}]OTf (**3**). To a solution of **1** (200 mg, 0.197 mmol) in dichloromethane (10 mL) was added an excess of **L**₁ (130 mg, 0.298 mmol). Immediately the color turned from pale yellow to deep reddish violet. After stirring 5 h at room temperature, the solution was evaporated to dryness to leave a violet solid, which was washed with diethyl ether and *n*-hexane. Yield: 86%. Anal. Found: C, 63.43; H, 4.14; S, 2.25. C₇₆F₃H₅₇O₆P₃ReS requires: C, 63.64; H, 4.00; S, 2.23. UV–visible: λ_{max}/nm (CH₂Cl₂) 561.32 (ε/dm³ mol⁻¹ 20015).

[(triphos)(CO)₂Re{C=C=C(Ph){μ-(*p*-C₆H₄)}C(Ph)(OH)(C≡CH)}]OTf (**4**). To a solution of **1** (200 mg, 0.197 mmol) in dichloromethane (10 mL) was added an excess of **L**₂ (100 mg, 0.295 mmol). Immediately the color turned from pale yellow to deep reddish violet. After stirring 3 h at room temperature, the solution was evaporated to dryness to leave a violet solid, which was washed with diethyl ether and *n*-hexane. Yield: 88%. Anal. Found: C, 61.43; H, 4.17; S, 2.58.

C₆₈H₅₅F₃O₆P₃ReS requires: C, 61.12; H, 4.15; S, 2.39. UV–visible: λ_{max}/nm (CH₂Cl₂) 555.27 (ε/dm³ mol⁻¹ 19709).

trans-[(dppe)₂ClRu{C=C=C(bianth)C(OH)(C≡CH)}]-(OTf) (5). To a solution of **2** (200 mg, 0.185 mmol) in dichloromethane (10 mL) was added an excess of **L**₁ (161 mg, 0.369 mmol). Slowly the color turned from orange-red to dark reddish violet. After stirring 24 h at room temperature, the solution was evaporated to dryness to leave a violet solid, which was washed with diethyl ether and *n*-hexane. Yield: 91%. Anal. Found: C, 68.00; H, 4.95; S, 2.21. C₈₅H₆₆ClF₃O₄P₄-RuS requires: C, 68.04; H, 4.40; S, 2.13. UV–visible: λ_{max}/nm (CH₂Cl₂) 511.98 (ε/dm³ mol⁻¹ 18321).

trans-[(dppe)₂ClRu{C=C=C(Ph)}{μ-(*p*-C₆H₄)}C(Ph)(OH)(C≡CH)}]OTf (6). To a solution of **2** (200 mg, 0.185 mmol) in dichloromethane (10 mL) was added an excess of **L**₂ (125 mg, 0.369 mmol). Slowly the color turned from pale yellow to deep purple. After stirring 24 h at room temperature, the solution was evaporated to dryness to leave a violet solid, which was washed with diethyl ether and *n*-hexane. Yield: 90%. Anal. Found: C, 65.44; H, 4.79; S, 2.55. C₇₇H₆₄ClF₃O₄P₄-RuS requires: C, 65.93; H, 4.56; S, 2.28. UV–visible: λ_{max}/nm (CH₂Cl₂) 512.96 (ε/dm³ mol⁻¹ 16998).

[(dppe)₂ClRu{C=C=C(bianth)C=C=C}RuCl(dppe)₂]-OTf)₂ (**7**). To a solution of **5** (200 mg, 0.133 mmol) in dichloromethane (10 mL) was added a stoichiometric amount of **2** (144 mg, 0.133 mmol). After stirring 11 days at room temperature the reaction was completed (³¹P{¹H} NMR monitoring). The solvent was evaporated to dryness in vacuo, and the deep violet solid was washed with diethyl ether and *n*-hexane. Yield: 83%. Anal. Found: C, 64.87; H, 4.65; S, 2.56. C₁₃₈H₁₁₂Cl₂F₆O₆P₈Ru₂S₂ requires: C, 64.60; H, 4.40; S, 2.49%. UV–visible: λ_{max}/nm (CH₂Cl₂) 573.16 (ε/dm³ mol⁻¹ cm⁻¹ 24831).

[(dppe)₂ClRu{C=C=C(bianth)C=C=C}Re(CO)₂-(triphos)]OTf)₂ (**8**). **Method A.** To a solution of **5** (200.0 mg, 0.133 mmol) in dichloromethane (10 mL) was added a stoichiometric amount of **1** (135 mg, 0.133 mmol). After stirring 9 days at room temperature the reaction was completed (³¹P NMR monitoring). The solvent was evaporated in vacuo, and the deep violet solid was washed with diethyl ether. Yield: 77%. **Method B.** To a solution of **3** (200.0 mg, 0.139 mmol) in dichloromethane (10 mL) was added a stoichiometric amount of **2** (150.9 mg, 0.139 mmol). After stirring 9 days at room temperature the reaction was completed (³¹P NMR monitoring). The solvent was evaporated in vacuo, and the deep violet solid was washed with diethyl ether. Yield: 73%. Anal. Found: C, 62.17; H, 4.18; S, 2.61. C₁₂₉H₁₀₃Cl F₆O₆P₇ReRuS₂ requires: C, 62.01; H, 4.15; S, 2.56%. UV–visible: λ_{max}/nm (CH₂Cl₂) 560.19 (ε/dm³ mol⁻¹ cm⁻¹ 12190).

[(dppe)₂ClRu{C=C=C(Ph){μ-(*p*-C₆H₄)}(Ph)C=C=C}-RuCl(dppe)₂](OTf)₂ (**9**). To a solution of **6** (200 mg, 0.142 mmol) in dichloromethane (10 mL) was added a stoichiometric amount of **2** (154 mg, 0.142 mmol). After stirring 4 days at room temperature the reaction was completed (³¹P NMR monitoring). The solvent was evaporated in vacuo, and the deep violet solid was washed with diethyl ether and *n*-hexane. Yield: 79%. Anal. Found: C, 64.87; H, 4.65; S, 2.56. C₁₃₀H₁₁₀-Cl₂F₆O₆P₈Ru₂S₂ requires: C, 64.60; H, 4.40; S, 2.49. UV–visible: λ_{max}/nm (CH₂Cl₂) 517.64 (ε/dm³ mol⁻¹ cm⁻¹ 24869).

[(dppe)₂ClRu{C=C=C(Ph){μ-(*p*-C₆H₄)}(Ph)C=C=C}Re-(CO)₂(triphos)]OTf)₂ (**10**). **Method A.** To a solution of **6** (200 mg, 0.142 mmol) in dichloromethane (10 mL) was added a stoichiometric amount of **1** (145 mg, 0.142 mmol). After stirring 6 days at room temperature the reaction was completed (³¹P NMR monitoring). The solvent was evaporated in vacuo, and the deep violet solid was washed with diethyl ether. Yield: 78%. **Method B.** To a solution of **4** (200 mg, 0.150 mmol) in dichloromethane (10 mL) was added a stoichiometric amount of **2** (162 mg, 0.150 mmol). After stirring 6 days at room temperature the reaction was completed (³¹P NMR monitoring). The solvent was evaporated in vacuo, and the deep violet

solid was washed with diethyl ether and *n*-hexane. Yield: 75%.
Anal. Found: C, 60.87; H, 4.55; S, 3.09. C₁₂₁H₁₀₁ClF₆O₈P₇-
ReRuS₂ requires: C, 60.53; H, 4.24; S, 3.05%. UV-visible:
 $\lambda_{\text{max}}/\text{nm}$ (CH₂Cl₂) 524.57 ($\epsilon/\text{dm}^3 \text{ mol}^{-1} \text{ cm}^{-1}$ 20000).

Acknowledgment. P.Z. gratefully acknowledges the financial support from the University of Siena (PAR 2003).
OM0492193